Article

J. Mex. Chem. Soc. **2024**, *68*(4)
Special Issue

ISSN-e 2594-0317

Biopanning Phage Display Libraries in Homogeneous Solution for Identification of Biomineralization Peptides of TiO_2

Armin Hernández-Gordillo[1,2], Andrés Hernández-Arana[1], L. Irais Vera-Robles[1*]

[1]Departamento de Química, Área de Biofisicoquímica, Universidad Autónoma Metropolitana-Iztapalapa, San Rafael Atlixco 186, Col. Vicentina, 09340, CDMX, México.
[2]Centro de Investigación en Nanociencias y Nanotecnología, Centro Universitario de los Valles, Carretera Guadalajara-Ameca Km. 45.5, Ameca, Jalisco, C.P. 46600, México.

***Corresponding author:** L. Irais Vera-Robles, email: irrob@xanum.uam.mx

Received April 30th, 2024; Accepted August 12th, 2024.

DOI: http://dx.doi.org/10.29356/jmcs.v68i4.2262

Abstract. Peptides and proteins rich in positively charged residues have been the most frequently reported for TiO_2 biomineralization since their identification is based on peptide screening on its negatively charged surface. To achieve optimum interaction of the peptides with the biomimetic synthesis precursors rather than interaction with the final product, in this work, a selection of peptides with biomineralization activity was proposed by performing a biopanning directly on the precursor Titanium(IV) bis(ammonium lactate) dihydroxide (TiBALDH). Using two phage display libraries (12- and 7-mer) in different buffer systems, four possible sequences with biomineralization activity of TiO_2 were identified: TNWQALAYMQRH (TN), ENHWSLSTLMSS (EN), GLHTSATNLYLH (GL), TWYPNRPPILEL (TW). The selection of buffer and concentration of TiBALDH were vital for a reliable identification. Synthetic peptides with sequences TN and EN, were selected for *in vitro* biomineralization of TiO_2. Both peptides were able to form anatase nanoparticles at room temperature. However, the EN sequence showed lower activity than TN, specially in acetate buffer, requiring a higher concentration to initiate biomineralization. These changes in reactivity can be attributed principally to different states of protonation of the residues mainly due to the glutamic acid in EN. Although the secondary structure determined by circular dichroism results in disordered chains, a common motif could be identified between the two peptides -pol-pol-W-pol-x-x-x-x-M-, where the W and M residues match. The results provide new possibilities for using combinatorial techniques to find new biological templates for nanomaterial synthesis.
Keywords: Phage display; peptides; titanium oxide; biopanning; biomineralization.

Resumen. Péptidos y proteínas ricas en residuos con carga positiva han sido frecuentemente reportados para la biomineralización de TiO_2, ya que su identificación se basa en la detección de péptidos sobre su superficie con carga negativa. Para alcanzar una interacción óptima del péptido con el precursor biomimético, en lugar de la interacción con el producto final, en este trabajo, se propuso realizar un biotamizado empleando el precursor dihidroxilactatotitanato(IV) de bis-amonio (TiBALDH) para seleccionar péptidos con actividad de biomineralización. Empleamos dos librerías de fago desplegado (12 y 7 residuos) en diferentes soluciones amortiguadoras, identificando cuatro posibles secuencias con actividad biomineralizante de TiO_2: TNWQALAYMQRH (TN), ENHWSLSTLMSS (EN), GLHTSATNLYLH (GL), TWYPNRPPILEL (TW). La elección del amortiguador y la concentración de TiBALDH fueron vitales para una selección confiable. Los péptidos sintéticos TN y EN, fueron escogidos para la biomineralización de TiO_2 *in vitro*. Ambos péptidos fueron capaces de formar nanopartículas de anatasa a temperatura ambiente, sin embargo, la secuencia EN mostró menor actividad que TN, especialmente en amortiguador de acetatos, requiriendo una concentración mayor para iniciar la biomineralización. Estas diferencias de reactividad pueden ser atribuidas principlamente a los estados de

J. Mex. Chem. Soc. **2024**, *68*(4)
Special Issue

ISSN-e 2594-0317

protonación de los residuos de ácido glutámico en EN. Aunque la estructura secundaria determinada por dicroísmo circular mostró cadenas desordenadas, se identificó un motivo común entre los dos péptidos—pol-pol-W-pol-x-x-x-x-M-, donde los aminoácidos W y M coinciden. Los resultados abren nuevas posibilidades para usar técnicas combinatorias para hallar nuevas plantillas biológicas para la síntesis de nanomateriales.
Palabras clave: Fagos desplegados; péptidos; óxido de titanio; bioselección; biomineralización.

Introduction

In nature, biomolecules (DNA, lipids, peptides, and proteins) are responsible for using the available resources around them to guide the synthesis of inorganic materials, by a process called biomineralization. Proteins or peptide motifs that can biomineralize silica, nacre, bones, nanoparticles among others, have been found in several organisms [1-4]. Albeit some helpful inorganic structures are produced by distinct proteins; which have been identified and sequenced, other materials with relevant technological applications, such as TiO_2 are not produced naturally by biomolecules [5].

For this reason, several efforts have been made to find sequences with biomineralizing activity for non-biogenic materials. For example, microorganisms have been used to introduce titanium precursors into their metabolism to synthesize TiO_2 nanostructures, but this method does not provide information on the biomolecules involved in biomineralization [6,7].

Alternatively, the combinatorial technique known as biopanning allows the selection of peptides that bind specifically to a target [8]. In particular, the M13 phage display library consists of a collection of phages genetically engineered to express random amino acid sequences (between 7 and 12 residues) on solvent-exposed regions of protein site p3, which have been widely used to find peptides with affinity to a specific target [9]. Thus, the affinity of millions of different sequences can be tested in a single experiment. Mostly, the screening experiments are done against the material of interest; however, although some selected peptides show an affinity for specific oxides, they are necessarily not the best template to induce the formation of a particular structure from a precursor [10].

For example, making the biopanning on TiO_2 surfaces a great number of peptide sequences have been proposed for biomineralizing TiO_2 nanoparticles in their different crystalline phases and shapes [11-13]. However, some of these peptides did not exhibit biomineralizing activity and there is not a clear correlation between the role of each amino acid in biomineralization [11]. Some authors suggest that positive charges, *eg.* arginine or lysine residues, are necessary to interact electrostatically with the negative charge of the oxide and their charge seems to be closely related to the biomineralization yield of TiO_2 [11,14,15]. However, a few peptides without these positive charge residues have been reported [16,17], either as isolated motifs or as building blocks attached to other platforms, to be capable of producing controlled TiO_2 crystalline structures. Accordingly, the sequence with an affinity to the surface of the material is not the unique factor that ensures the biomineralizing [18].

Therefore, to identify of sequences with biomineralizing activity, it is necessary to perform biopanning directly on the molecular precursors instead of on a solid phase. Żelechowska *et al.* has tested this hypothesis, modifying the biopanning approach, selecting peptides that, in the presence of a precursor, can bind it and further induce the formation of a given inorganic material, *eg.* ZnO [19]. As well this approach has been helpful in finding peptides with catalytic activity for organic reactions [20]. Thus, biopanning on a molecular target can be a promising route for finding specific peptides to biomineralize TiO_2.

In this work, we proposed to use an alternative target. Instead of using TiO_2 (final material), we employed the precursor titanium(IV) bis(ammonium lactate)dihydroxide (TiBALDH), which is water soluble. It has been reported that this precursor coexists with TiO_2 nanoparticles in the equilibrium, and it shifted toward its production can be guided by experimental parameters such as solvent polarity and solution dilution, among others [21]. Accordingly, in a previous work, we investigated its stability also in different buffers, presence of ions and pH [22]. Then, TiBALDH was used to identify sequences that have biomineralization activity and affinity to the final material. Thus, if TiO_2 particles are formed, it will be indicated that there are phages with sequences that catalyze the reaction, which may also interact with the particles formed. These phages can be recovered from the aqueous solution by centrifugation, and, after DNA sequencing, the peptide sequence attached to TiO_2 can be known. With this methodology, it can be assured that the sequences obtained from biopanning have biomineralization activity with

J. Mex. Chem. Soc. **2024**, *68*(4)
Special Issue

ISSN-e 2594-0317

TiBALDH, thus minimizing the requirement of a positive charge on the precursor. Once the sequences were deciphered, these two peptides were tested for TiO_2 biomineralization at room temperature to demonstrate that this methodology can be applied to find specific sequences that may work on biomineralization using other precursors.

Experimental

Biopanning in homogeneous phase

The biopanning to identify TiO_2 binding peptides was performed according to the protocol recommended by the manufacturer of the phage display libraries (New England BioLabs, Ph. D. Phage Display Libraries). Phage display libraries of 7- and 12-mer were used, modifying the section of the target material. An acidic, a neutral, and a basic buffer solution (sodium acetate pH 4.5, sodium phosphate pH 7.0, and Tris buffer pH 8.0) were chosen, and deionized water was a negative control. In brief, ~10^{11} phages were added to 500 µL of TiBALDH (Sigma Aldrich, stored at 4 °C) 50 mM in the respective buffer. The mixed solution was placed at room temperature for 5 days to ensure the interaction of the peptides exposed on p3 proteins with the titanium precursor and consequent TiO_2 biomineralization. After incubation, the solution was centrifuged (14 000 rpm, 10 min), washed and phage eluted according to the New England Biolabs protocol. In each round of biopanning, the eluate was amplified and titrated for subsequent clone selection (20 for each experiment). DNA sequencing was performed by Eurofins MWG Operon (Louisville, KY). Three panning rounds were performed.

Biomineralization of TiO_2 using peptides

The peptide sequences were selected from biopanning results. Two peptides, TN (TNWQALAYMQRH) and EN (ENHWSLSTLMSS) (purity ≥ 96 %) were synthesized by Biomatik (USA). A stock solution of each peptide of 5.0 mg/mL was prepared in sterile deionized water. Solutions of TiBALDH 50 mM in Tris or acetate buffer (100 mM) were prepared with different peptide concentrations. After incubation for 24 h, the solution was recovered by centrifugation (14 000 rpm, 10 min), washed once with the corresponding buffer solution, and dried at room temperature. The biomineralized TiO_2 was characterized by dispersion light scattering (Zetasizer Nano, Malvern Panalytical), transmission electron microscopy (JEOL 2010 operated to 200 KeV), and Fourier Transform infrared spectroscopy (Spectrum GX, Perkin Elmer) equipped with ATR. To monitor the content of Ti in the biomineralization process, soluble Ti(IV) was quantified by colorimetry using Tiron (4,5-dihydroxy-1,3-benzenedisulfonic acid) [23]. Briefly, 10 µL of the titanium sample was added to 190 µL of Tiron 5 mM in acetate buffer. The mixture was incubated at room temperature for 2 h, and then the UV-vis absorption spectrum was acquired (NanoDrop 2000). The percentage of Ti(IV) was calculated with the absorption ratio (at 380 nm), assuming the absorption of TiBALDH in water at the same molar concentration was 100 %.

Circular dichroism

Circular dichroism (CD) spectra in the 250-190 nm region were registered with a JASCO J-715 instrument (Jasco Inc., Easton, MD) using a 1.00-mm- path length cell. Peptides were dissolved in water at concentrations ca. 0.1 mg/mL (pH ca. 6.7) and spectra were recorded at 25.0 °C. Spectral raw data were transformed to mean residue ellipticity [θ].

Results and discussion

Biopanning

Biopanning was performed using three buffered media (pH 4.5, pH 7.0, and pH 8.0) and deionized water as a negative control. Both 12- and 7-mer phage display libraries were tested to study the effect of peptide length on biopanning. In the first step, the phage display library was put in contact with the TiBALDH solution (50 mM) and incubated for a few days (Fig. 1**(a)**). Several days were necessary to guarantee the specific interaction, reaching of the equilibrium, and biomineralization of TiO_2 on the p3 protein (Fig. 1**(b)**). Phage-TiO_2 conjugates were recovered

J. Mex. Chem. Soc. **2024**, *68*(4)
Special Issue

ISSN-e 2594-0317

by centrifugation since phage alone did not precipitate at 14000 rpm (Fig. 1**(c)**). Finally, the eluate was plated to verify that phages with probable biomineralizing activity were recovered. This procedure was repeated twice.

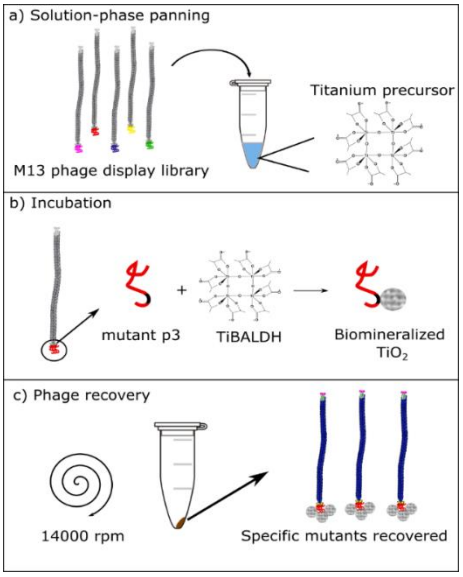

Fig. 1. Scheme biopanning procedure in homogeneous solution with TiBALDH as a target.

Interestingly, after the first biopanning cycle with TiBALDH, the results were similar with both 12- and 7-mer libraries (Table 1). For the negative control and the acetate buffer (pH 4.5), it was not possible to recover phages (no plaques were detected); this implies that the interaction of M13 mutants with the titanium precursor under those conditions was not adequate to induce TiO_2 biomineralization. A possible explanation is that the negative charge of TiBALDH is repelled by the phage, which is also negative. Also, it is known that small TiO_2 nanoparticles can be redissolved in citrate buffer, probably both factors hampering its production in detectable amounts. On the contrary, as was expected phages were recovered (plaques were clearly visible on the *E. coli* lawn) in phosphate and tris buffer. Indeed, it has been reported that phosphates promote the formation of TiO_2 nanoparticles in the presence of TiBALDH; however, they are trapped inside of their nanoparticles as a contaminant [16]. Conversely, Tris buffer does not react with TiBALDH; according to our size measurements, no shifts were detected, while phosphates increase dramatically its size from units to hundreds of nm as reported before [22]. Then, Tris buffer should allow phages with specific interaction and/or biomineralizing activity to be rescued by centrifugation, forming plaques, as shown in Table 1.

Table 1. Phages recovered after the first round of biopanning in TiBALDH (50 mM) in the selected buffers (100 mM).

Buffer	**pH**	**Plaques after 1st biopanning cycle***
Acetate	4.5	No
Water	7.0	No
Phosphate	7.0	Yes
Tris	8.0	Yes

* The results correspond to both 12- and 7-mer phage display libraries.

J. Mex. Chem. Soc. **2024**, *68*(4)
Special Issue

ISSN-e 2594-0317

Since no plaques were obtained in acetate and water systems, the second biopanning cycle was not continued in those systems. Three rounds were completed with phosphate and Tris buffer, and phages were recuperated, eluted, and plated. To identify the sequences, we selected 20 clones in each experiment of the 7-mer biopanning. For the 12-mer library, 20 and 40 plaques for PB and Tris were selected, respectively all clones found are shown in Table 2.

Table 2. Sequences found in biopanning experiments of TiBALDH.

Plaque	**Sequence**			
	12-mer library		**7-mer library**	
	PB	**Tris**	**PB**	**Tris**
1	TWYPNRPPILEL	ISGPWASYAIGP	WT	WT
2	FEDPRTWWVTHL	WT	TGFHLTM	WT
3	TNWQALAYMQRH	WAKDPSWKVRGN	YEPYKRI	WT
4	VSNKMPDGENWR	GLHTSATNLYLH	QILVHKN	WT
5	SLNGPIHRLLKT	IPLGRDGGSYQR	FHPRTTS	WT
6	GWYAASGTSLLS	GYSFIDPPRKFH	QGYGVPT	TPTAPVR
7	WT	AIWPKTELFLIS	TTPLSHR	WT
8	ENHWSLSTLMSS	WT	GRLDTGI	WT
9	TFYLVNPGSRLG	RPDIQLLPNSWA	HNIKETH	WT
10	GLHTSATNLYLH	GLHTSATNLYLH	LRSDPVV	WT
11	TTKFPPFVSVLS	VASRIHPLGIDP	DSSLFAL	GMHETHV
12	TWYPNRPPILEL	QLLPGLLKEHVQ	WT	WT
13	ENHWSLSTLMSS	TLPAILQSSGTR	WT	WT
14	SLRWPVAVHHSN	KGSLDARLLSR	YLGFDVH	WT
15	VSLSGVSSNSRV	TNWQALAYMQRH	SRPPVPA	WT
16	DWSSWVYRDPQT	WT	IKHPFGF	FASRSDT
17	SGVYKVAYDWQH	-	SPNYNII	YGAKNNL
18	TLSDWGYGNFRA	WT	GMLSDGR	QYYSFDH
19	DWSSWVYRDPQT	GVLHNLTAATSL	ASTLIVF	TPPlVWT
20	VFSSMVHVLNTH	VPVSNVWPWRPE	IHANWSP	NIPSLPF
21	-	GTGLVTLPRLTV	-	-
22	-	WT	-	-

J. Mex. Chem. Soc. **2024**, *68*(4)
Special Issue

ISSN-e 2594-0317

Plaque	Sequence			
	12-mer library		7-mer library	
	PB	Tris	PB	Tris
23	-	GDLLTFQNFVMK	-	-
24	-	TNWQALAYMQRH	-	-
25	-	DWSSWVYRDPQT	-	-
26	-	SQDIRTWNGTRS	-	-
27	-	DWSSWVYRDPQT	-	-
28	-	SILDGWLVVDSS	-	-
29	-	DWSSWVYRDPQT	-	-
30	-	DWSSWVYRDPQT	-	-
31	-	VPSWFFANWGPS	-	-
32	-	GFYSNLVGSINV	-	-
33	-	DWSSWVYRDPQT	-	-
34	-	DWSSWVYRDPQT	-	-
35	-	TDSPTSQRQPYG	-	-
36	-	DWSSWVYRDPQT	-	-
37	-	DWSSWVYRDPQT	-	-
38	-	DWSSWVYRDPQT	-	-
39	-	DWSSWVYRDPQT	-	-
40	-	DWSSWVYRDPQT	-	-

WT: wild-type phage. In red and green are indicated W and M, respectively, and the motif that is shared is underlined.

The 12-mer library gave 5 sequences that were repeated at least once. Table 3 contains the sequences most frequently found in the 12-mer library experiments. The most frequent sequence was DW (DWSSWVYRDPQT), found in both experiments (phosphate and Tris). At first sight, the DW peptide could be considered as a sequence capable of promoting TiO_2 formation from TiBALDH, but in combinatorial techniques such as biopanning, it is common to find false positives. A literature search found that this sequence has been reported with affinity to several systems, including polypropylene (the material of the tubes used in biopanning) [24,25].

Thus, the most frequent sequence DW was discarded in addition to GLHTSATNLYLH, which has also been found in some experiments but does not present similarity with the system studied here [26-28]. Therefore, the sequences considered for biomineralization experiments were TN (TNWQALAYMQRH) and EN (ENHWSLSTLMSS) because of the contrasting isoelectric points. It should be noted that despite this dissimilar charge, a sequence alignment carried out with [29] Clustal Omega showed that, although the similarity was not high, peptides EN and TN share a common motif that can be represented as follows: -pol-

J. Mex. Chem. Soc. **2024**, *68*(4)
Special Issue

ISSN-e 2594-0317

pol-W-pol-x-x-x-x-M-, where pol and x denote polar and any amino acids, respectively. The two coincident residues, W and M, have hydrophobic characteristics that could serve as the stabilizers of the nanoparticle aggregates, while the hydrophilic motif -pol-pol- at one end would be responsible for interacting electrostatically with the titanium complex. This motif can be used as a starting point for the design of peptides with high yield in TiO_2 biomineralization. Another reason for choosing EN and TN peptides was to try not to use sequences with R or K in the central positions of the peptide [11].

It is important to note that when the alignment analysis was performed among all the 12-mer peptides found in the biopanning, it is observed that the DW peptide has a coincidence respect to the TN in residues W and Y. Thus, we do not ignore the possible biomineralizing activity of DW and further experiments are needed to establish this correlation between aromatic residues.

With respect to the 7-mer peptides found in biopanning, did not have consensus sequence. Furthermore, the alignment does not show any matching motifs with peptides EN and TN, which is the reason why 7-mer peptides were being discarded for this job. However, the align analysis shows that peptides LRSDPVV, and SRPPVPA have a motif -S-pol-P-apol-V-; where pol and apol means polar and nonpolar respectively, and peptides QILVHKN, and TTPLSHR match in residues L and H, making them good candidates for future research.

Table 3. Most frequent sequences found in biopanning experiments.

Peptide	Frequency	Sequence	Buffer	pI*
DW	13	DWSSWVYRDPQT	PB and Tris	4.47
TN	3	TNWQALAYMQRH	PB and Tris	9.06
GL	3	GLHTSATNLYLH	PB and Tris	7.38
TW	2	TWYPNRPPILEL	PB	6.25
EN	2	ENHWSLSTLMSS	PB	5.50

*Isoelectric point (pI) was calculated using the Protein Calculator [30]. Where red and green letter shows the same amino acid.

Structural characterization of EN and TN peptides

Circular dichroism spectra of the selected peptides in the far-UV region are shown in Fig. 2, where it can be seen that the most salient feature is the intense negative peak *ca*. 200 nm, with [θ] between 13,000 and 19,000 deg cm^2 $dmol^{-1}$. It is known that such intense negative CD bands appear in spectra of short lysine- and proline-rich peptides [31] and have been attributed to some content of polyproline II conformation in those peptides. However, this spectral shape is also similar to that corresponding to the unordered or coil structural type described in a CD spectral basis used for the analysis of peptide CD spectra [32].

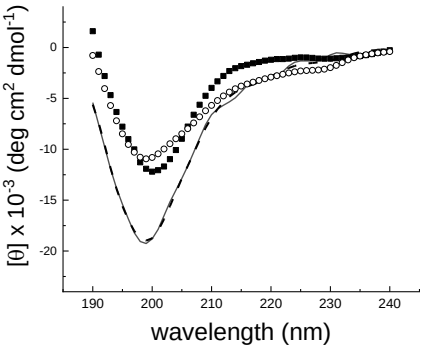

Fig. 2. CD spectra of EN (solid line) and TN (squares) peptides in water, pH *ca*. 7.0. Calculated spectra reconstructed from results of analysis by the CONTIN-LL algorithm are shown as dashed lines for EN and circles for TN.

J. Mex. Chem. Soc. **2024**, *68*(4)
Special Issue

ISSN-e 2594-0317

Quantitative estimations of the secondary structures of EN and TN were carried out using two well-known algorithms used for protein secondary structure determinations: CONTIN-LL (implemented in the online server DichroWeb) [33] and BeStSel [34]. Further analysis was performed employing an unconstrained linear combination of basis spectra for typical secondary structures in peptides [32]. For both of the peptides, the three methods gave concordant results (Table 4) indicating coil (unordered) structure as the most abundant, followed by beta strands. However, the contents of turns were rather variable.

Overall, analyses of CD spectra seem to point to the presence of a few residues in beta-strand conformation in both EN and TN, and the major number of residues in unordered (irregular structure).

Table 4. Predictions of secondary structure from circular dichroism spectra.

Peptide	Method	Helix	Beta	Turns	Coil (unordered)
EN	BeStSel	3	31	19	48
EN	Contin	5	17	14	64
EN	Multiple linear regresion	6	21	0	72
TN	BeStSel	0	39	21	40
TN	Contin	6	22	15	56
TN	Multiple linear regresion	0	0.37	0.04	0.60

Biomineralization of TiO_2 using the selected peptides

Thus, the two peptides, namely TN and EN, were used for biomineralization experiments, although EN was found in phosphate buffer, it was also employed in Tris buffer for comparison purposes. Although at pH 8.0 the TN peptide is positively charged and the EN peptide is negatively charged (Fig. 3), no difference was observed in the biomineralization product, suggesting that the reaction does not depend on the protonation state of the basic residues (R and H).

In Tris buffer, both EN and TN peptides were able to biomineralize TIBALDH at ≥ 2.0 mg/mL concentrations. Considering that EN peptide did not emerge in Tris, a low biomineralization activity was expected under these conditions. However, Fig. 3 shows how both TN and EN peptides at 2.0 mg/mL caused a similar increase in particle size. The particles of 3 nm present in TiBALDH solution are related to the equilibrium between titanium lactate polymers probably caping a TiO_2 core [21]. In presence of peptides the chemical equilibrium is modified due to the molecular interaction between carboxylic groups, and hydrogen bonds, probably by forming micelle-type arrangements [35]. The biomineralization products were analyzed by TEM (Fig. 4), where nanoparticles with crystalline planes corresponding to the anatase phase are observed with both peptides. The difference between the sizes obtained by DLS and TEM can be explained by the formation of electrostatically stabilized agglomerates.

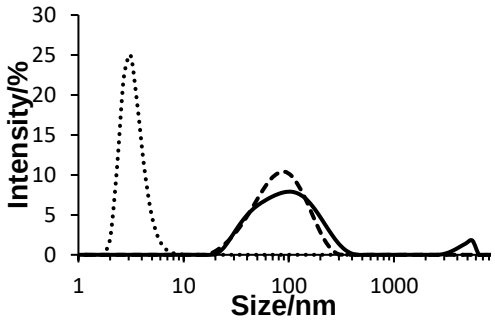

Fig. 3. Size particle distribution of TiBALDH (50 mM) alone in Tris buffer (dotted line), and after addition of TN peptide (dashed line) and EN peptide (continuous line).

J. Mex. Chem. Soc. **2024**, *68*(4)
Special Issue

ISSN-e 2594-0317

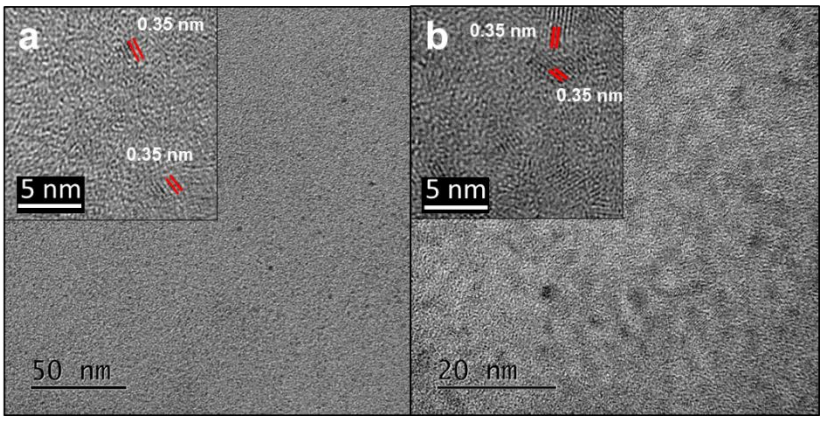

Fig. 4. TEM images of TiO_2 nanoparticles biomineralized from TiBALDH in Tris buffer and the peptides **(a)** TN and **(b)** EN.

The influence of pH and protonation states were studied using the acetate buffer. When peptides in the presence of acetates are mixed with TIBALDH, an evident increase in the biomineralization product is observed. Both peptides generate a precipitate whose size makes its characterization impossible by DLS. In acetate buffer, the TN peptide could precipitate TiO_2 even at concentrations of 0.5 mg/mL while the EN peptide caused precipitation at concentrations ≥ 2.0 mg/mL.

To determine the percentage of biomineralized TiO_2, the amount of soluble titanium (TiBALDH) was quantified (Fig. 5). In the case of the TN peptide (originally found in Tris buffer biopanning), the amount of remaining TiBALDH was 32 and 26 % in Tris and acetate buffer, respectively, these values are similar to those peptides joined to proteins [19] whose activity is larger than isolated peptides. The acetate buffer, in the absence of peptide, also decreases the soluble Ti(IV); the low pH and the presence of carboxylic groups can be responsible of this behavior [21]. On the contrary, EN peptide shows percentages of remanent TiBALDH of 82 and 40% in Tris and acetate buffer, respectively more similar to values reported by other groups for isolated peptides [11, 16]. The lower biomineralization activity of the EN peptide could be explained since this sequence was not specific to that medium. In the case of acetate medium, considering that the isoelectric point (pI) of EN peptide is 5.5, at pH 4.5 it has a lower positive charge than the TN peptide, thus its activity in acidic environments could be related to the protonation state of the more acidic residues.

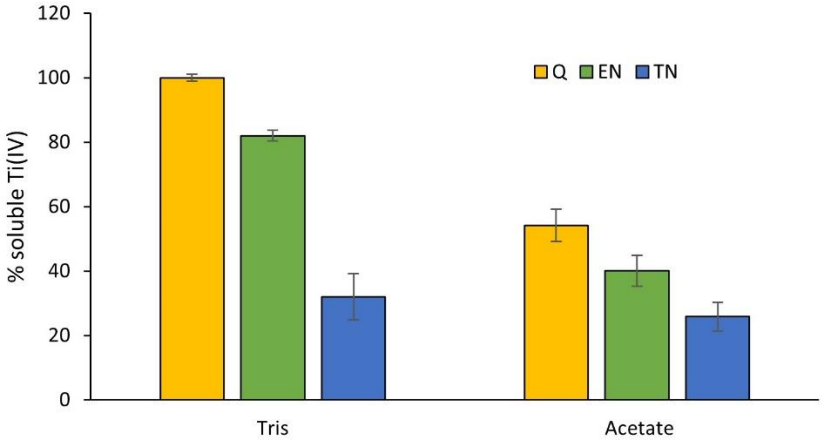

Fig. 5. Percentage of TiBALDH remaining after biomineralization for each peptide (EN in green and TN in blue) in Tris buffer and acetate buffer and negative control in absence of peptides (Q in yellow).

J. Mex. Chem. Soc. **2024**, *68*(4)
Special Issue

ISSN-e 2594-0317

The peptide residues that change their protonation state from pH 8.0 (Tris) to 4.5 (acetate) are glutamate and histidine for EN and histidine for TN. Because both peptides contain histidine, therefore the protonation state of glutamate is probably what influences the difference in reactivity between peptides. At pH 4.5 the Glu residue in EN is protonated and could cause a decrease in biomineralization activity because few carboxylate groups are available to coordinate with the titanium species. A study of the molecular dynamics of peptides may also help explain their reactivity in terms of flexibility and accessibility to their functional groups.

Finally, the infrared spectra of the oxides obtained with the EN and TN peptides are shown in Fig. 7, where the characteristic band of the Ti–O bonds is below the $\tilde{\nu}$ 800 cm^{-1}. It is also observed that the samples prepared in the presence of Tris present a band in $\tilde{\nu}$ 1045 cm^{-1} that corresponds to C–O bonds in alcohols, which is possibly due to the remaining molecules from the buffer.

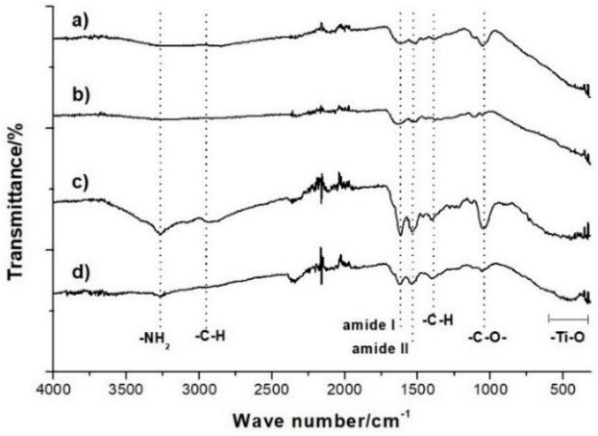

Fig. 7. FTIR spectra of TiO_2 biomineralized in the presence of TN and EN peptide in distinct buffers. TN-TiO_2 in Tris **(a)** and acetate **(b)** buffers. EN-TiO_2 in Tris **(c)** and acetate buffers **(d)**. EN-TiO_2 is the material prepared with EN peptide and TN-TiO_2 corresponds to TN peptide.

In all samples, bands associated with the peptide are present; specifically, amide I bands appearing in the region of intermolecular beta structures ($\tilde{\nu}$ 1610–1625 cm^{-1}) are possibly caused by the interaction of the peptide with the surface of TiO_2. Although the intensity of amide bands varies depending on the sample, the most intense ones were observed for EN, which would imply a better affinity of EN for TiO_2. However, despite having a high affinity for TiO_2, EN displays low biomineralizing activity.

Based on the above results, it can be concluded that the identification of peptides with biomineralizing activity with a particular precursor is feasible for TiO_2. However, the results demonstrate the importance of having a specific sequence for each buffered medium since the EN peptide was not found in Tris Buffer; although biomineralization activity is observed, it shows a poor efficiency. In addition, caution must be maintained when selecting peptides because of false positives. The type of material of the vessel where biopanning takes place should not interfere with phage selection.

Conclusions

Solution-phase biopanning using a phage display library and TiBALDH as a TiO_2 precursor was proposed as an alternative method to identify sequences with biomineralizing activity. Using a 7-residue library it was not possible to identify consensus sequences, while in the 12-residue library, the sequences TNWQALAYMQRH (TN), ENHWSLSTLMSS (EN), GLHTSATNLYLH (GL), TWYPNRPPILEL (TW) were found at least twice. TN and EN peptides were tested for TiO_2 biomineralization using the precursor

J. Mex. Chem. Soc. **2024**, *68*(4)
Special Issue

ISSN-e 2594-0317

TiBALDH; both peptides presented activity in 0.1 M Tris (pH 8.0) medium producing crystalline TiO_2 nanoparticles of ~ 5 nm at room temperature. At pH 4.5 in acetate buffer, the EN sequence was less active than TN, requiring a higher concentration to initiate biomineralization. These pH-dependent changes of reactivity can be attributed to the different states of protonation of the peptides, and mainly to the glutamic acid in EN. Furthermore, the effect of the peptide conformation on its biomineralizing capacity can be ruled out since both peptides seemingly display unordered conformations in solution. A biopanning methodology using precursors instead of the target material would be applied as a more convenient approach to directly find sequences with biomineralization activity.

Acknowledgments

We thank Laboratorio de Microscopía Electrónica de La Universidad Autónoma Metropolitana-Iztapalapa and Patricia Castilo for sample analysis.

References

1. Heintze, C.; Babenko, I.; Suchanova, J. Z.; Skeffington, A.; Friedrich, B. M.; Kröger, N. *Proc. Natl. Acad. Sci.* **2022**, *119*, e2211549119. DOI: https://doi.org/10.1073/pnas.2211549119.
2. Otter, L.M.; Eder, K.; Kilburn, M.R. *et al. Nat. Commun.* **2023**, *14*, 2254. DOI: https://doi.org/10.1038/s41467-023-37814-0.
3. Sharma, V.; Srinivasan, A.; Nikolajeff, F.; Kumar, S. *Acta Biomaterialia*. **2021**, *120*, 20-37. DOI: https://doi.org/10.1016/j.actbio.2020.04.049.
4. Liu, F.; Shah, D. S.; Gadd, G. M. *Curr. Biol.* **2021**, *31*, 358-368. DOI: https://doi.org/10.1016/j.cub.2020.10.044.
5. Buettner, K. M.; Valentine, A. M. *Chem. Rev.* **2011**, *112*, 1863-1881.
6. Jha, A. K.; Prasad, K.; Kulkarni, A. R. *Colloids Surf. B.* **2009**, *71*, 226-229. DOI: https://doi.org/10.1016/j.colsurfb.2009.02.007.
7. Lang, Y.; Monte, F. D.; Rodriguez, B. J.; Dockery, P.; Finn, D. P.; Pandit, A. *Sci. Rep.* **2013**, *3*, 3205. DOI: 10.1038/srep03205.
8. Smith G. P.; Petrenko V. A. *Chem. Rev.* **1997**, *97*, 391–410. DOI: https://doi.org/10.1021/cr960065d.
9. Bratkovič T. *Cell. Mol. Life Sci.* **2010**, *67*, 749-767. DOI: https://doi.org/10.1007/s00018-009-0192-2.
10. 10. Rosant, C.; Avalle, B.; Larcher, D.; Dupont, L.; Fribouleta, A.; Tarascon, J.-M. *Energy Environ. Sci.* **2012**, *5*, 9936–9943. DOI: https://doi.org/10.1039/C2EE22234E.
11. Dickerson, M. B.; Jones, S. E.; Cai, Y.; Ahmad, G.; Naik, R. R.; Kröger, N.; Sandhage, K. H. *Chem. Mater.* **2008**, *20*, 1578-1584. DOI: https://doi.org/10.1021/cm071515t.
12. Sun, Y.; Tan, J.; Wu, B.; Wang, J.; Qu, S.; Weng, J.; Feng, B. *Colloids Surf. B.* **2016**, *146*, 307-317. DOI: https://doi.org/10.1016/j.colsurfb.2016.06.032.
13. Chen, H.; Su, X.; Neoh, K.-G.; Choe, W.-S. *Anal. Chem.* **2006**, *78*, 4872-4879. DOI: https://doi.org/10.1021/ac0603025.
14. Park, S.; Lee, H.; Lee, S.-Y. *Dalton Trans.* **2013**, *42*, 13817-13820. DOI: https://doi.org/10.1039/C3DT51040A.
15. Liu, C.; Jiang, Z.; Tong, Z.; Li, Y.; Yang, D. *RSC Adv*. **2014**, *4*, 434-441. DOI: https://doi.org/10.1039/C3RA44630A.
16. Puddu, V.; Slocik, J. M.; Naik, R. R.; Perry, C. C. *Langmuir*. **2013**, *29*, 9464–9472. DOI: https://doi.org/10.1021/la401777x.
17. Hellner, B.; Stegmann, A. E.; Pushpavanam, K.; Bailey, M. J.; Baneyx F. *Langmuir*. **2020**, *36*, 8503–8510. DOI: https://doi.org/10.1021/acs.langmuir.0c01108.

J. Mex. Chem. Soc. **2024**, *68*(4)
Special Issue

ISSN-e 2594-0317

18. Choi, N.; Tan, L.; Jang, J.-r.; Um, Y.M.; Yoo, P.J.; Choe, W.-S. *J. Inorg. Biochem.* **2012**, *115*, 20-27. DOI: https://doi.org/10.1016/j.jinorgbio.2012.05.011.
19. Zelechowska, K.; Karczewska-Golec, J.; Karczewski, J.; Los, M.; Klonkowski, A. M.; Wegrzyn, G.; Golec, P. *Bioconjugate Chem.* **2016**, *27*, 1999–2006. DOI: https://doi.org/10.1021/acs.bioconjchem.6b00196.
20. Maeda, Y.; Javid, N.; Duncan, K.; Birchall, L.; Gibson, K. F.; Cannon, D.; Kanetsuki, Y.; Knapp, C.; Tuttle, T.; Ulijn, R. V.; Matsui. H. *J. Am. Chem. Soc*. **2014**, *136*, 15893−15896. DOI: https://doi.org/10.1021/ja509393p.
21. Seisenbaeva, G. A.; Daniel, G.; Nedelec, J.-M.; Kessler, V. G. *Nanoscale*. **2013**, *5*, 3330. DOI: https://doi.org/10.1039/C3NR34068F.
22. Hernández-Gordillo, A.; Hernández-Arana, A.; Campero-Celis, A.; Vera-Robles, L.I. *RSC Adv*. **2019**, *9*, 34559-34566. DOI: https://doi.org/10.1039/C9RA05923G.
23. Moharir, A.V.; Sarma, V.A.K.; Krishna Murti G.S.R. *Microchem. J.* **1972**, *17*, 167-172. DOI: https://doi.org/10.1016/0026-265X(72)90169-5.
24. Hu, Y.-F.; Gao, X.-C.; Xu, T.-Q.; Dun, Z.; Yu, X.-L. *Comb. Chem. High Throughput Screening*. **2016**, *19*, 283-289.
25. Vodnik, M.; Zager, U.; Strukelj, B.; Lunder, M. *Molecules.* **2011**, *16*, 790-817. DOI: https://doi.org/10.3390/molecules16010790.
26. Majerova, P.; Hanes, J.; Olesova, D.; Sinsky, J.; Pilipcinec, E.; Kovac, A. *Molecules.* **2020**, *25*, 874. DOI: https://doi.org/10.3390/molecules25040874.
27. Nemudraya, A. A.; Kuligina, E.V .; Ilyichev, A. A.; Fomin, A. S.; Stepanov, G. A.; Savelyeva, A.V.; Koval, O.A.; Richter, V.A. *Oncol. Lett.* **2016**, *12*, 4547-4555. DOI: https://doi.org/10.3892/ol.2016.5266.
28. Zhang, H.; Guo, Z.; He, B.; Dai, W.; Zhang, H.; Wang, X.; Zhang, Q. *Adv. Healthc. Mater*. **2018**, *7*, 1800269. DOI: https://doi.org/10.1002/adhm.201800269.
29. Clustal Omega https://www.uniprot.org/align/clustalo-R20220708-213026-0610-21074307-p1m, accessed in July 2022.
30. http://protcalc.sourceforge.net/, accessed in January 2022
31. Rucker, A.L.; Creamer T.P. *Protein Sci.* **2002**, *11*, 980-985 doi: 10.1110/ps.4550102.
32. Reed, J,; Reed T. A. *Anal Biochem.* **1997**, *254*, 36-40 https://doi.org/10.1006/abio.1997.2355.
33. (a)Whitmore, L.; Wallace, B. A. *Nucleic Acids Res.* **2004**, *32*, W668–W673. DOI: https://doi.org/10.1093/nar/gkh371. (b)Whitmore, L.; Wallace, B.A. *Biopolymers* **2008**, *89*, 392–400. DOI: https://doi.org/10.1002/bip.20853. (c)http://www.cryst.bbk.ac.uk/cdweb, accessed in June 2022. (d)Sreerama, N.; Woody, R.W. *Anal. Biochem.* **2000**, *287*, 252–260.
34. Micsonai, A.; Wien, F.; Bulyáki, É.; Kun, J.; Moussong, É.; Lee, Y.-H.; Goto, Y.; M.; Réfrégiers, Kardos, J. *Nucleic Acids Research* **2018**, *46*, W315 W322. DOI: https://doi.org/10.1093/nar/gky497. http://bestsel.elte.hu.
35. Hernández-Gordillo, A.; Hernández-Arana, A.; Campero, A.; Vera-Robles, L.I. *Langmuir*. **2014**, *30*, 4084-4093. DOI: https://doi.org/10.1021/la500203k.